A calibrated multi-scale 14 ka lacustrine earthquake record from the Eastern Alps, Austria - validating seismic hazard curves

Christoph Daxer[(1)], Jyh-Jaan Steven Huang[(1)], Yin Lu[(1)], Stefan Weginger[(2)], Michael Hilbe[(3)], Michael Strasser[(1)], Jasper Moernaut[(1)]

[(1)]University of Innsbruck, Austria [(2)]ZAMG - Central Institute for Meteorology and Geodynamics, Austria [(3)]University of Bern, Switzerland

Seismotectonic setting and seismic hazard assessment in Austria

Our study region is the state of Carinthia (southern Austria, bordering Italy and Slovenia; Fig. 1). The seismotectonic environment of this area is governed by the counterclockwise rotation of the Adriatic microplate, which causes N-S directed convergence of ~2-3 mm/yr. The convergence is accommodated by i) the indentation of the relatively rigid Adriatic microplate into the European plate; ii) uplift in the Eastern Alps and iii) eastward extrusion of the Pannonian fragment (Fig. 1a & b; Brückl et al., 2010; Serpelloni et al., 2016). These processes lead to seismicity along major strike-slip faults in the Eastern Alps and the Dinaric system and along thrust faults in the Southern Alps (Friuli), resulting in a comparably high seismic hazard in Carinthia (Fig. 1).

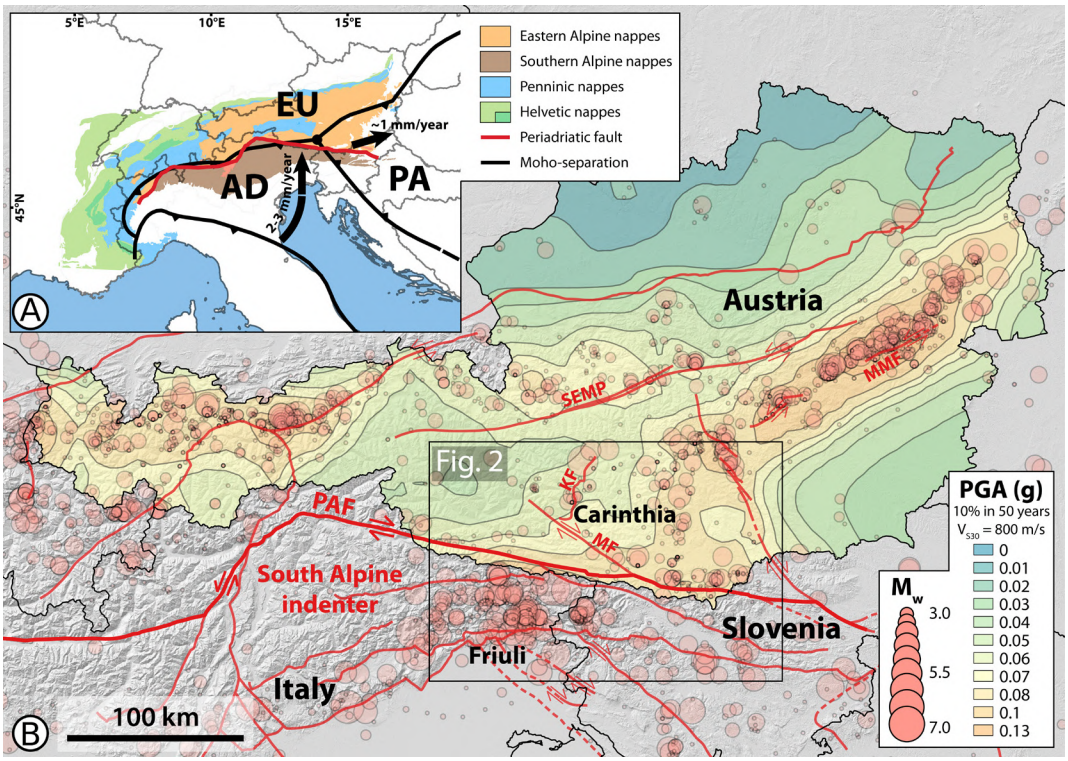

***Figure 1**: **A** Tectonic map (simplified after Schmid et al., 2004) and crustal structure of the Alps (modified after Brückl et al., 2010; Faccenna et al., 2004). Arrows indicate relative motion of the Adriatic plate (AD) and the Pannonian fragment (PA) relative to the European plate (EU). **B** Current seismic hazard map of Austria (Weginger et al., 2019). KF: Katschberg normal fault, MF: Mölltal fault, MMF: Mur-Mürz fault, PAF: Periadriatic fault, SEMP: Salzach-Ennstal-Mariazell-Puchberg fault. Earthquake locations and M_w are plotted according to the Austrian earthquake catalogue (ZAMG, 2021).*

The probabilistic seismic hazard analysis (PSHA) in Austria is based on the Austrian earthquake catalogue (ZAMG, 2021), complemented by the catalogue of the International Seismological Centre (ISC, 2022). The magnitude-frequency model is built on events with M ≤ 5 (local intensities ≤ V at the studied lake) and extended to an M_{max} of ~6.5 estimated via the EPRI approach (Coppersmith et al., 2012). Presumably, even stronger earthquakes (estimated M up to ~7; Fig. 2) affected the study area in historical time. Due to insufficient catalogue completeness and unclear epicentres, these are not considered by PSHA, thus adding some uncertainty to the validity of seismic hazard curves.

Episodic, clustered and migrating seismicity is often observed in intraplate areas (Stein et al., 2015) and might lead to phases of enhanced seismic hazard. It is therefore crucial to test the seismic hazard maps created via PSHA with long, calibrated paleoseismic archives and assess the interevent times and recurrence patterns of strong earthquakes.

Here, we reveal the long-term earthquake recurrence in Carinthia using a ~14 ka long paleoseismic record from Wörthersee and compare it to the seismic hazard curves derived from PSHA.

FWF Der Wissenschaftsfonds. Interreg Italia-Österreich European Regional Development Fund. EUROPEAN UNION. AP OMIA. universität innsbruck

Studied lake and field data acquisition

Wörthersee (*See* = german for lake)

- glacigenic lake
- area = 19 km2
- max. depth = 84 m
- divided into several depositional areas
- affected by strong (I_L > V) earthquake shaking in 1976, 1857, 1690, 1511 and 1348

Studied via

- bathymetric mapping
- high-resolution seismic data (3.5 kHz and 8 kHz)
- 26 short (1.5 m) and 8 long (~11 m) sediment cores

→ possibility to identify and map landslide deposits and turbidites induced by earthquakes in great detail

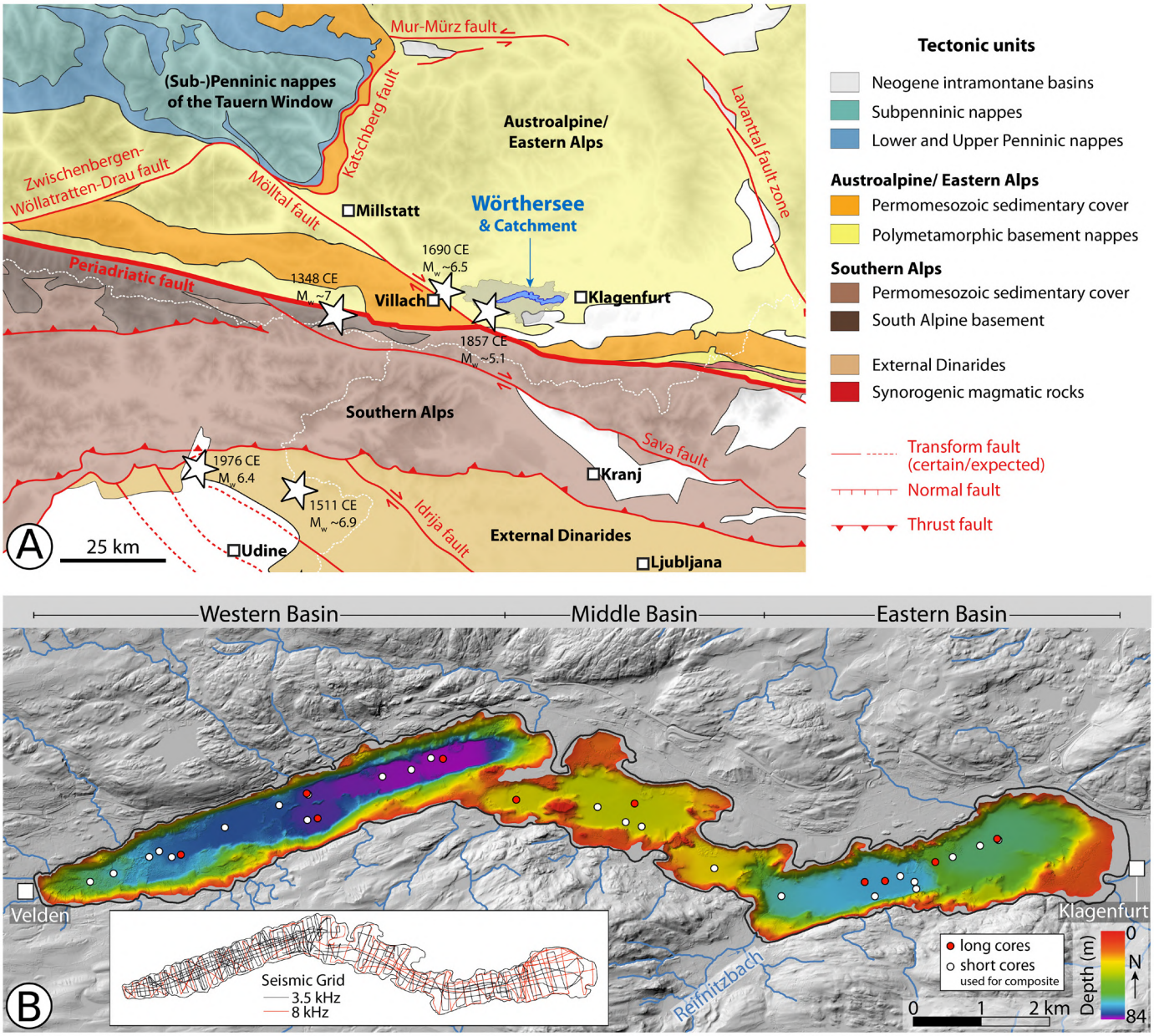

***Figure 2**: Overview of the study area. **A** Seismotectonic setting (simplified from Reinecker & Lenhardt 1999; Schmid et al. 2004; Reiter et al. 2018). IF: Idrija fault, LFZ: Lavanttal fault zone, MF: Mölltal fault MM: Mur-Mürz fault, SF: Sava fault. Earthquake epicentres and magnitudes of the strongest earthquakes in the area were compiled from SHEEC 1000-1899 (Stucchi et al., 2013), SHEEC 1900-2006 (Grünthal et al., 2013) and the Austrian earthquake catalogue (ZAMG, 2021). **B** Bathymetric map of Wörthersee. Coring locations are indicated as red (long Kullenberg cores) and white (short percussion cores) dots. Each coring location has a specific intensity threshold for recording earthquakes, given in roman numerals (cf. Daxer et al., 2022). Different depositional areas are outlined in white (simplified after Daxer et al., 2022). In the lower left, the acquired reflection seismic grid using two different seismic sources is shown.*

Core analysis and identification of event deposits

- **Sediment core analysis** at the Austrian core facility (University of Innsbruck) by i) detailed macro- and microscopic description, ii) high-resolution magnetic susceptibility (2 mm step size), iii) γ-density (5 mm) measurements and iv) very high-resolution (0.2 to 1 mm step size) X-ray fluorescence measurements.

- **Identification of turbidites** based on i) their homogeneous or fining-upward macroscopic appearance, ii) peaks in Ca or Ti due to their composition and iii) their colour, which contrast to the finely laminated hemipelagic background sediment

- **Core-to-core correlation** of time-correlative turbidites ("events") and background sediment

- Confirmed by **AMS ^{14}C dating** carried out on terrestrial macro-remains from different short and long cores

- Inferring an **earthquake trigger confidence level** (ETCL) of event deposits based on the "synchronicity criterion" (e.g. Moernaut et al., 2014; Praet et al., 2017; Schnellmann et al., 2002) and turbidite composition

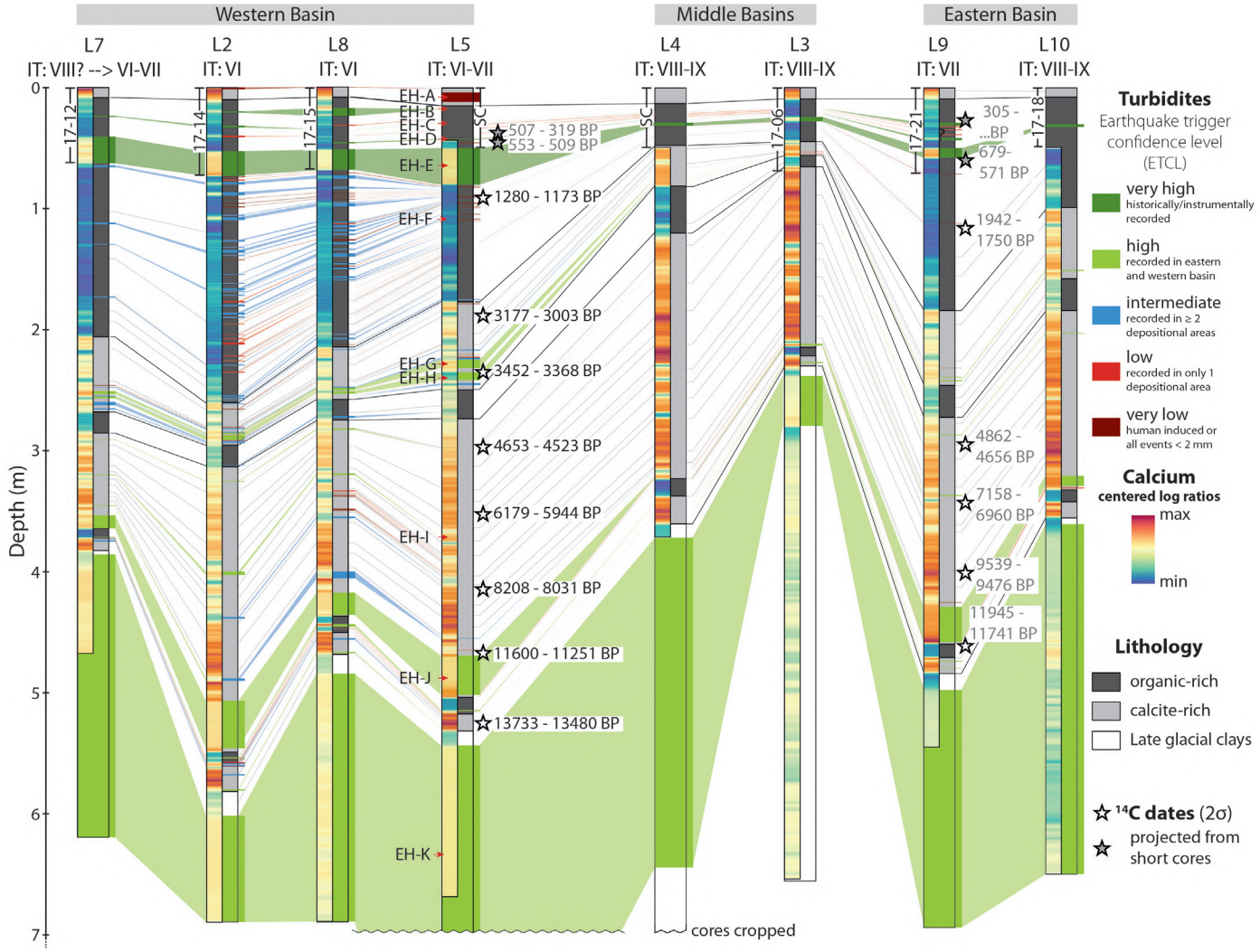

***Figure 3**: Correlation and general lithology of long sediment cores in Wörthersee. Depending on the distribution of turbidites, we assign an earthquake trigger confidence level to each turbidite-interval. The background-sedimentation of Wörthersee can be divided into three main lithologies: i) partly laminated dark organic-rich sediments with relatively low amount of calcite; ii) laminated calcite-rich sediments and iii) grey, laminated late glacial clays and silts (cf. Daxer et al. 2020). As indicated by the distribution of Calcium in the sediment (blue to red palette), the organic-rich sediments are mainly present in the upper part of the sediment cores. The Ca-rich sediments occupy an intermediate position in the cores and are followed downcore by late-glacial clays.*

Calibration of the turbidite record with historical earthquake data

Daxer et al. (2022) investigated the **imprints of the well-known historical earthquakes** of 1976, 1857, 1690, 1511 and 1348 CE (Fig. 4). Based on the presence or absence and the thickness of deposits caused by these earthquakes, they inferred **site-specific intensity recording thresholds** and established **size scaling relationships** of earthquake imprints vs. seismic intensity (Fig. 5).

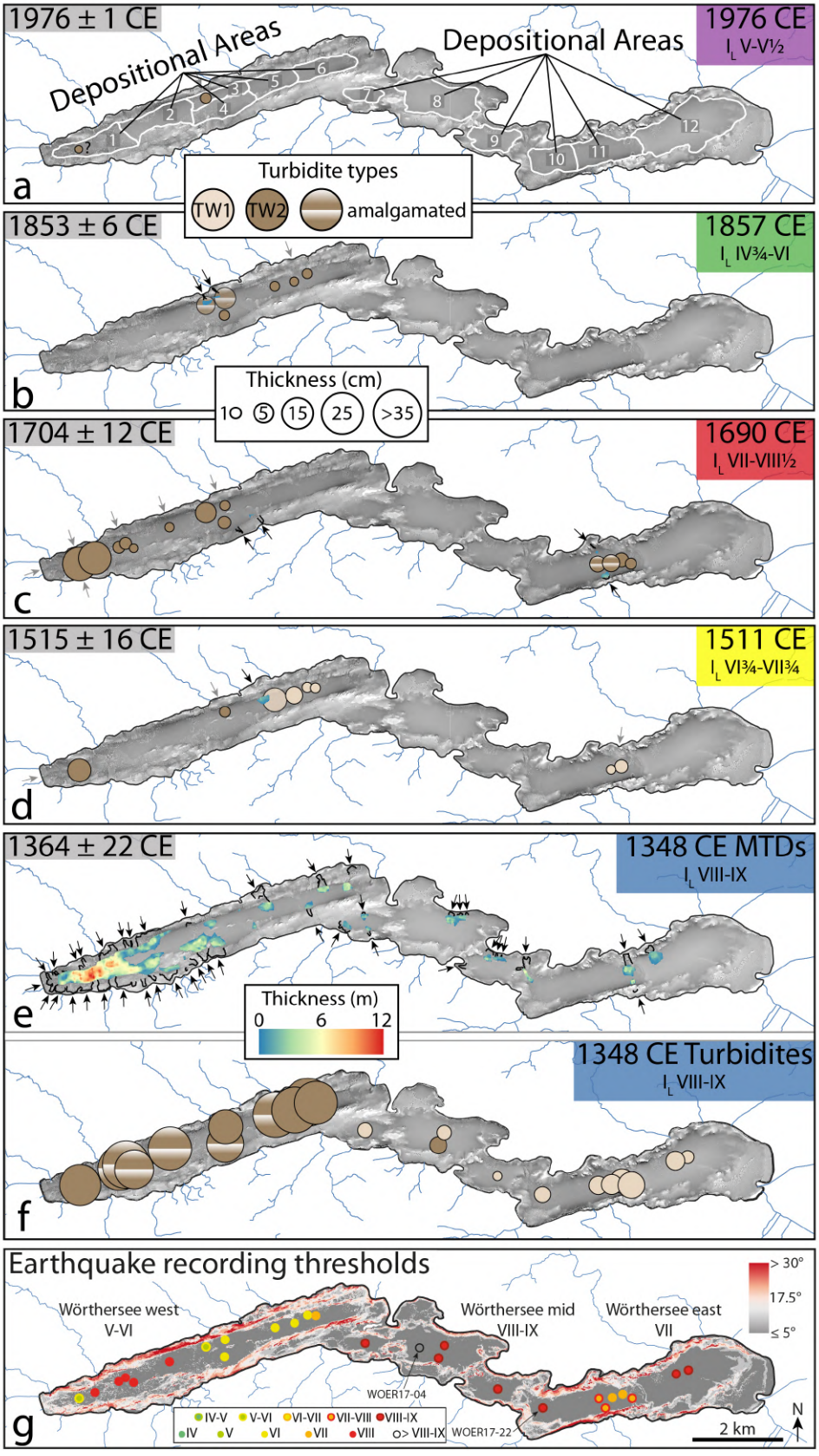

***Figure 4**: Spatial imprint of synchronous event deposits in Wörthersee, corresponding to the main earthquakes, and site-specific earthquake-recording thresholds (from Daxer et al., 2022). Individual subaqueous slope failures are denoted by arrows. Grey arrows indicate slope failures that could not be mapped in the bathymetric or seismic data but are inferred from the presence of turbidites in the sediment cores. a Imprint of the 1976 CE earthquake. Depositional areas are outlined in white. b Imprint of the 1857 CE earthquake. c Imprint of the 1690 CE earthquake. d Imprint of the 1511 CE earthquake. e MTDs caused by the 1348 CE earthquake. f Turbidites related to the 1348 CE earthquake. g Site-specific earthquake-recording thresholds derived from the presence or absence of sedimentary imprints related to earthquakes. Between the subbasins, the "general" EQRTs differ strongly (from V-VI to VIII-IX), depending on the depth of the respective subbasin. One coring site (WOER17-04), situated in the central middle basin, did not record any of the historical earthquakes, indicating a very high EQRT.*

Size-scaling relationships between earthquake imprint and seismic intensities

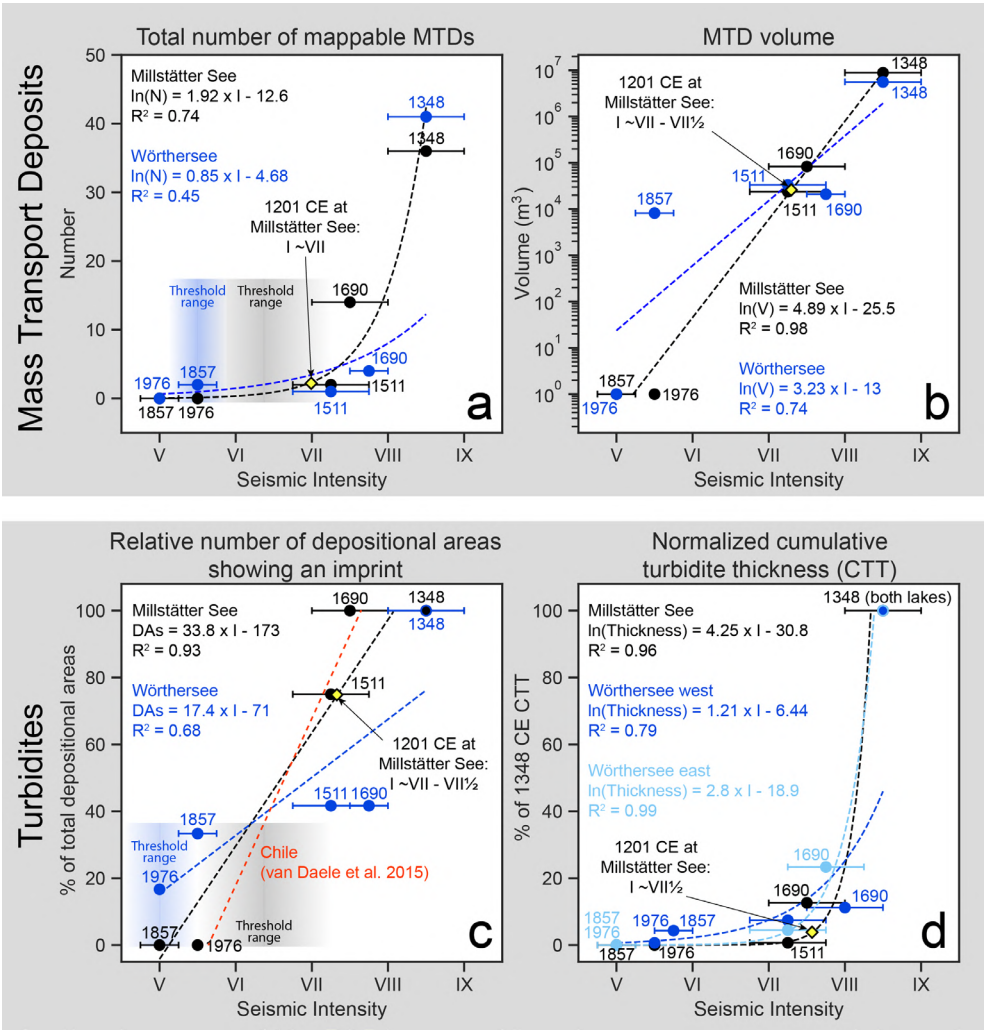

***Figure 5**: Size-scaling relationships of EQ imprint vs. seismic intensity derived by Daxer et al. (2022). Overall, the calibration curves underestimate mid-range intensities (VI-VIII) and overestimate low (<VI) and high (>VIII) intensities.*

***a** Seismic intensity vs. total number of mappable MTDs*

***b** Seismic intensity vs. MTD volume. The volume of remobilized sediment increases exponentially with seismic intensity.*

***c** Seismic intensity vs. relative number of depositional areas in a lake that record an earthquake. The higher the seismic intensity, the more depositional areas show an earthquake imprint.*

***d** Seismic intensity vs. normalized cumulative turbidite thickness (= the cumulated mean turbidite thicknesses per depositional area, normalized to the thickness of the AD1348 (mega-) turbidite).*

Applying the calibration - inferring intensities of prehistorical earthquakes

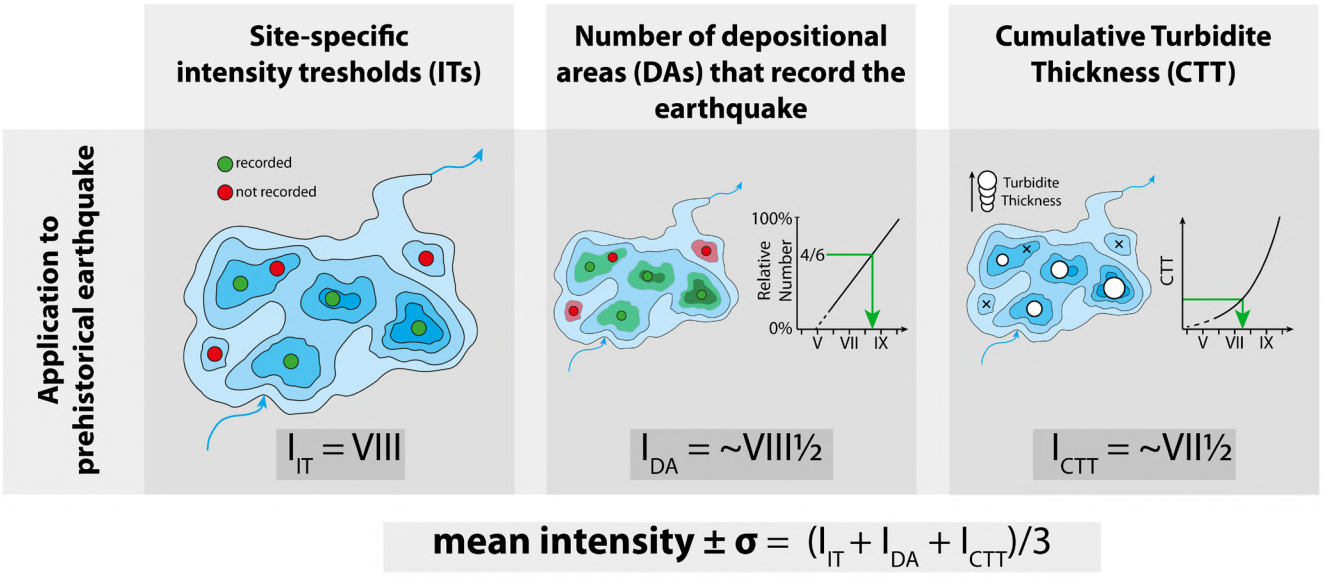

$$\textbf{mean intensity} \pm \sigma = (I_{IT} + I_{DA} + I_{CTT})/3$$

***Figure 6**: We use the site-specific intensity thresholds and the relationships between earthquake intensity and i) the relative number of depositional areas that record an earthquake and ii) the cumulative turbidite thickness provided by Daxer et al. (2022) to derive a "mean intensity" of prehistorical earthquakes recorded in the long sediment cores of Wörthersee.*

Intensities and temporal distribution of (prehistorical) earthquakes

- 44 event deposits fulfilling the synchronicity criterion → **44 earthquakes** recorded in the last ~14 ka
- Two intervals of **clustered earthquake occurrence** at 13.3 ka BP and 3.5 ka BP
- **Lithological change** and increased occurrence of earthquake-related event deposits from ~2.8 ka BP onwards
- → lowering of the earthquake recording threshold in unit III
- → calibration only valid for unit III, potential underestimation of intensities during unit II

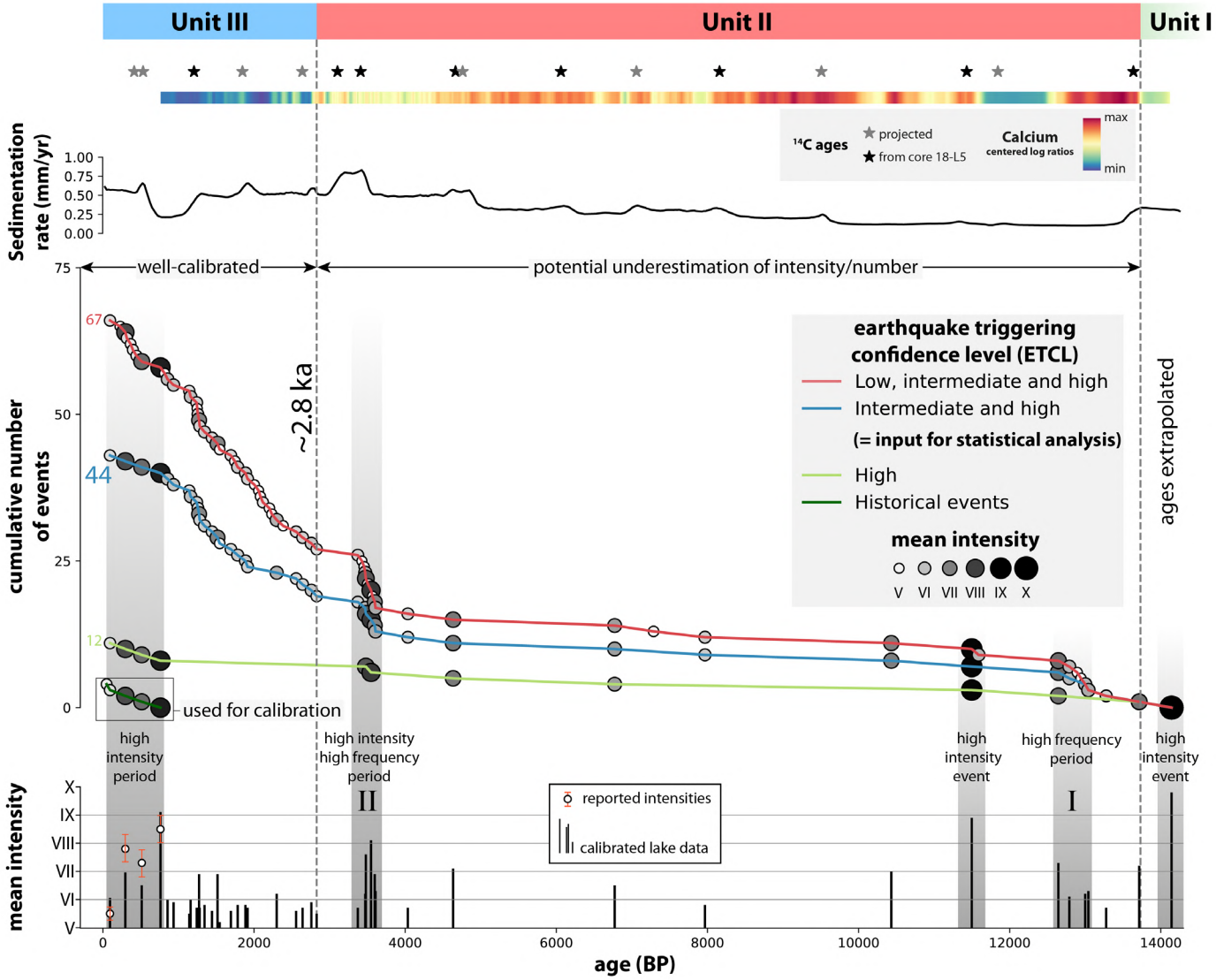

***Figure 7**: Temporal distribution of recorded events. The sedimentation rates derived from the age-depth models show a general increase towards the core top. 44 earthquakes of intermediate and high earthquake triggering confidence level are recorded in Wörthersee. Two phases of increased seismic activity (seismic bursts) are present in the event record spanning ~14,000 years.*

Recurrence statistics

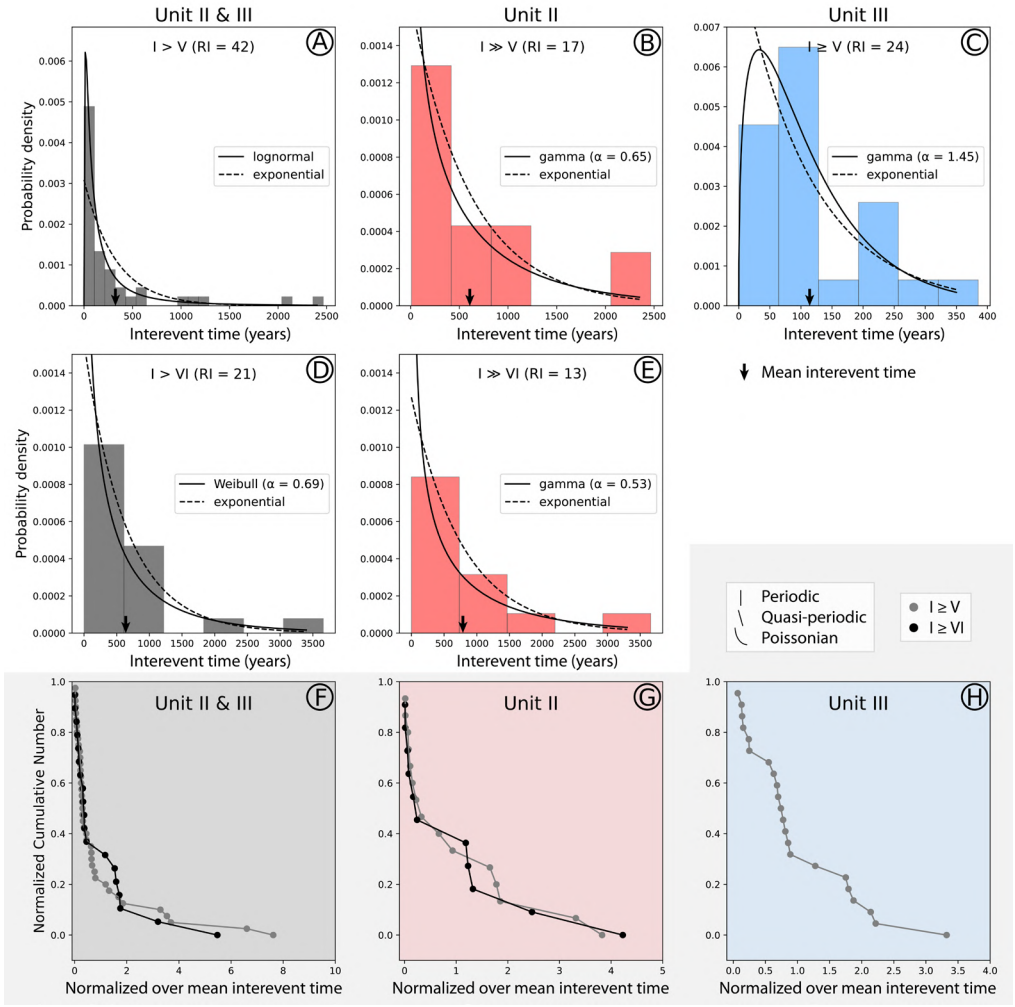

Complete dataset:
mean interevent time (mean ± stdev of interevent times) =
324 ± 536 years (I ≥ V)
639 ± 886 years (I ≥ VI)

Unit II:
608 ± 755 years (I ≥ V)
788 ± 1078 years (I ≥ VI).
Gamma distribution (α < 1)
→ bursty

Unit III:
114 ± 94 years (I ≥ V)
Gamma distribution (α > 1)
→ aperiodic or weakly periodic (confirmed by statistical tests)

***Figure 8**: Return time statistics of earthquakes (ETCL intermediate and high). **A-E** Histograms of interevent times for different observation intervals and intensity ranges. **F-H** Normalized recurrence data for different observation intervals for comparison to distribution shapes.*

Influence of age uncertainty

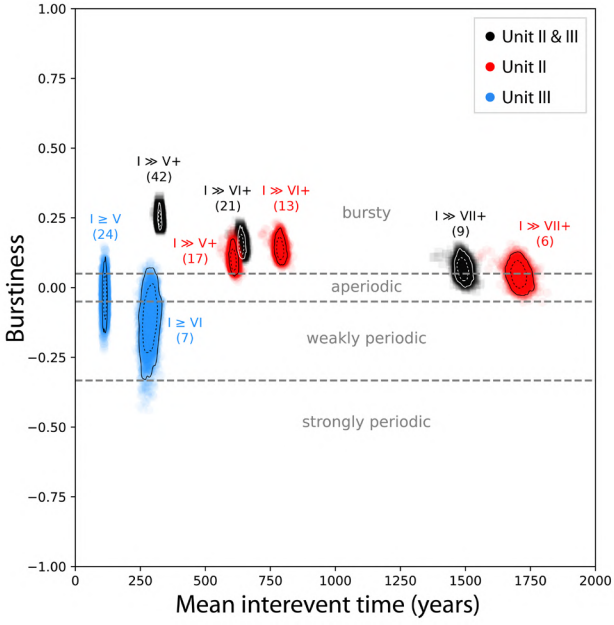

- 3586 age-depth-model iterations
- Unit II: bursty or aperiodic/bursty behaviour confirmed
- Unit III: aperiodic/weakly periodic pattern confirmed; age uncertainty plays a minor role (rather large *N* (24) for a paleoseismic record; cf. Kempf and Moernaut, 2021)

→ **Poissonian behaviour can be confidently attributed to the unit III, I ≥ V subset**

***Figure 9**: Interevent time vs. burstiness diagram of different subsets of the turbidite paleoseismic record from Wörthersee. Individual datapoints result from different age-depth model iterations (>3500 in total). Solid lines indicate 95% confidence intervals, dashed lines 68% confidence intervals. Numbers in brackets indicate the number of interevent times.*

Validating probabilistic seismic hazard curves with lacustrine data

Calculation of exceedance probability in 50 years (PoE_{50}) of a certain intensity I_x by dividing the number of recorded events in our lake record ($I \geq I_x$) by the record span

→ PoE_{50} decreases exponentially with seismic intensity
→ PoE_{50} of I ≥ V½ event in unit III: 40 % (well-calibrated)
→ PoE_{50} of I ≥ V½ event in unit II: 10 % (due to higher EQRT)
→ PoE_{50} of very high (> VIII) intensity events: ~1% (can only be inferred from unit II)

Testing the seismic hazard curve of the Wörthersee area provided by ZAMG (Weginger et al., 2019):

- Conversion of PGA values to intensity degrees using conversion formula given by (Faenza and Michelini, 2010) & comparison to PoE_{50} obtained from lake data (Fig. 10b)
- Lake data (I > 5) is complementary to instrumental and historical dataset used by PSHA (I < ~V)
- very good agreement between both datasets → **verification of the PSHA in the area of Wörthersee**

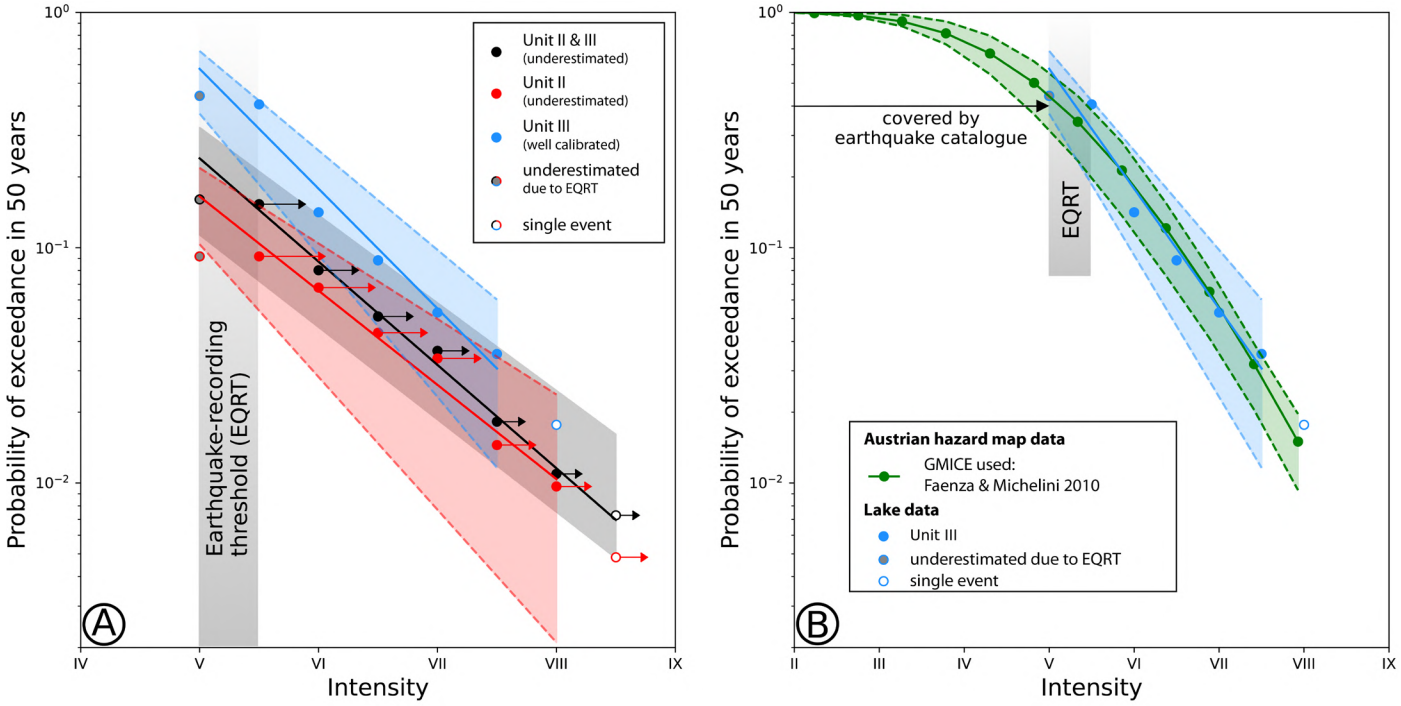

***Figure 10**: Seismic hazard curves. **A** Lake-derived probability of exceedance of certain intensities in 50 years. Arrows indicate underestimation of hazard for the combined (black) and unit II (red) dataset. **B** Comparison between the hazard curves derived from lacustrine data of unit III (blue) and the probabilistic seismic hazard assessment (green).*

Conclusions

In a recent publication (Daxer et al., 2022), we established size-scaling relationships between earthquake intensity and sedimentary imprints as well as and site-specific intensity thresholds based on five historically/instrumentally documented earthquakes in the south-eastern Alps. Here, we apply these calibration curves on a 14 ka long record from Wörthersee and draw the following conclusions:

- Poissonian earthquake recurrence, as used in PSHA, is confirmed for the last 2.8 ka
- The current seismic hazard curves of the study area are in agreement with the lacustrine paleoseismic record
- Intervals of enhanced earthquake frequency can occur and need to be considered in seismic hazard analysis
- Compared to the whole record, the last ~800 years show a relatively high number of strong intensity events

Acknowledgements

This work is funded by the Austrian Science Fund (FWF), project number P30285-N34, the Interreg V- Italy-Austria project *ARMONIA* (ITAT-301 6) and the Austrian Academy of Sciences project "S4SLIDE-Austria". Christoph Daxer acknowledges financial support from a research grant from the University of Innsbruck (Exzellenzstipendium für Doktoratskollegs).

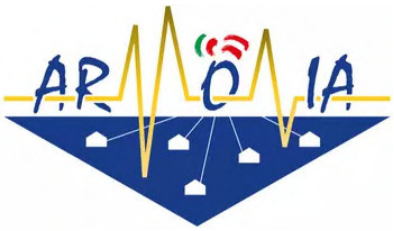

References

Brückl, E., Behm, M., Decker, K., Grad, M., Guterch, A., Keller, G.R., Thybo, H., 2010. Crustal structure and active tectonics in the Eastern Alps. Tectonics 29, n/a-n/a. https://doi.org/10.1029/2009TC002491

Coppersmith, K.J., Salomone, L.A., Fuller, C.W., Glaser, L.L., Hanson, K.L., Hartleb, R.D., Lettis, W.R., Lindvall, S.C., McDuffie, S.M., McGuire, R.K., others, 2012. Central and Eastern United States (CEUS) Seismic Source Characterization (SSC) for Nuclear Facilities.

Daxer, C., Ortler, M., Fabbri, S.C., Hilbe, M., Hajdas, I., Dubois, N., Piechl, T., Hammerl, C., Strasser, M., Moernaut, J., 2022. High-resolution calibration of seismically-induced lacustrine deposits with historical earthquake data in the Eastern Alps (Carinthia, Austria). Quat. Sci. Rev. 284, 107497. https://doi.org/10.1016/j.quascirev.2022.107497

Daxer, C., Sammartini, M., Molenaar, A., Piechl, T., Strasser, M., Moernaut, J., 2020. Morphology and spatio-temporal distribution of lacustrine mass-transport deposits in Wörthersee, Eastern Alps, Austria. Geol. Soc. London, Spec. Publ. 500, 235–254. https://doi.org/10.1144/SP500-2019-179

Faccenna, C., Piromallo, C., Crespo-Blanc, A., Jolivet, L., Rossetti, F., 2004. Lateral slab deformation and the origin of the western Mediterranean arcs. Tectonics 23. https://doi.org/10.1029/2002TC001488

Faenza, L., Michelini, A., 2010. Regression analysis of MCS intensity and ground motion parameters in Italy and its application in ShakeMap. Geophys. J. Int. 180, 1138–1152. https://doi.org/10.1111/j.1365-246X.2009.04467.x

International Seismological Centre, 2022. ISC-GEM Earthquake Catalogue. https://doi.org/10.31905/d808b825

Kempf, P., Moernaut, J., 2021. Age Uncertainty in Recurrence Analysis of Paleoseismic Records. J. Geophys. Res. Solid Earth 126, 1–16. https://doi.org/10.1029/2021JB021996

Moernaut, J., Van Daele, M., Heirman, K., Fontijn, K., Strasser, M., Pino, M., Urrutia, R., De Batist, M., 2014. Lacustrine turbidites as a tool for quantitative earthquake reconstruction: New evidence for a variable rupture mode in south central Chile. J. Geophys. Res. Solid Earth 119. https://doi.org/10.1002/2013JB010738

Praet, N., Moernaut, J., Van Daele, M., Boes, E., Haeussler, P.J., Strupler, M., **Schmidt**, S., Loso, M.G., De Batist, M., 2017. Paleoseismic potential of sublacustrine landslide records in a high-seismicity setting (south-central Alaska). Mar. Geol. 384, 103–119. https://doi.org/10.1016/j.margeo.2016.05.004

Reinecker, J., Lenhardt, W.A., 1999. Present-day stress field and deformation in eastern Austria. Int. J. Earth Sci. 88, 532–550. https://doi.org/10.1007/s005310050283

Reiter, F., Freudenthaler, C., Hausmann, H., Ortner, H., Lenhardt, W., Brandner, R., 2018. Active seismotectonic deformation in front of the Dolomites indenter, Eastern Alps. Tectonics 1–30. https://doi.org/10.1029/2017TC004867

Schmid, S.M., Fügenschuh, B., Kissling, E., Schuster, R., 2004. Tectonic map and overall architecture of the Alpine orogen. Eclogae Geol. Helv. 97, 93–117. https://doi.org/10.1007/s00015-004-1113-x

Schnellmann, M., Anselmetti, F.S., Giardini, D., McKenzie, J.A., Ward, S.N., 2002. Prehistoric earthquake history revealed by lacustrine slump deposits. Geology 30, 1131. https://doi.org/10.1130/0091-7613(2002)030<1131:PEHRBL>2.0.CO;2

Serpelloni, E., Vannucci, G., Anderlini, L., Bennett, R.A., 2016. Kinematics, seismotectonics and seismic potential of the eastern sector of the European Alps from GPS and seismic deformation data. Tectonophysics 688, 157–181. https://doi.org/10.1016/j.tecto.2016.09.026

Stucchi, M., Rovida, A., Gomez Capera, A.A., Alexandre, P., Camelbeeck, T., Demircioglu, M.B., Gasperini, P., Kouskouna, V., Musson, R.M.W., Radulian, M., Sesetyan, K., Vilanova, S., Baumont, D., Bungum, H., Fäh, D., Lenhardt, W., Makropoulos, K., Martinez Solares, J.M., Scotti, O., Živčić, M., Albini, P., Batllo, J., Papaioannou, C., Tatevossian, R., Locati, M., Meletti, C., Viganò, D., Giardini, D., 2013. The SHARE European Earthquake Catalogue (SHEEC) 1000–1899. J. Seismol. 17, 523–544. https://doi.org/10.1007/s10950-012-9335-2

Weginger, S., Jia, Y., Papi-Isaba, M., Lenhardt, W., Hausmann, H., 2019. Entwicklung einer regionalen Erdbebengefährdungskarte für Österreich in: Adam, C. Achs, G 27–34.

ZAMG, 2021. AEC - Austrian Earthquake Catalogue.